Article

Experimental Study on the Microstructural Characterization of Retardation Capacity of Microbial Inhibitors to Spontaneous Lignite Combustion

Yanming Wang [1,2,*], Ruijie Liu [1], Xiaoyu Chen [1], Xiangyu Zou [1], Dingrui Li [1] and Shasha Wang [1]

1   School of Safety Engineering, China University of Mining and Technology, Xuzhou 221116, China; ts23120035a31@cumt.edu.cn (R.L.); 5465@cumt.edu.cn (X.C.); ts22120234p31@cumt.edu.cn (X.Z.); ts23120025a31ld@cumt.edu.cn (D.L.); ts20120125p31@cumt.edu.cn (S.W.)
2   Intelligent Ventilation Research Center, China University of Mining and Technology, Xuzhou 221116, China
*   Correspondence: yanming.wang@cumt.edu.cn

Abstract: Mine fires are one of the common major disasters in underground mining. In addition to the external fire sources generated by mining equipment and mechanical and electrical equipment during operations, coal is exposed to air during mining, and spontaneous combustion is also the main cause of mine fires. In order to reduce the hidden danger of coal mines caused by spontaneous coal combustion during lignite mining, the microbial inhibition of coal spontaneous combustion is proposed in this paper. Via SEM, pore size analysis, and NMR and FT-IR experiments, the mechanism of coal spontaneous combustion is discussed and revealed. The modification of lignite before and after the addition of retardants is analyzed from the perspective of microstructure, and the change in flame retardancy of the lignite treated with two retardants compared with raw coal is explored. The results show that, compared with raw coal, a large number of calcium carbonate particles are attached to the surface of the coal sample after bioinhibition treatment, and the total pore volume and specific surface area of the coal sample after bioinhibition treatment are decreased by 68.49% and 74.01%, respectively, indicating that bioinhibition can effectively plug the primary pores. The results of NMR and Fourier infrared spectroscopy show that the chemical structure of the coal sample is mainly composed of aromatic carbon, followed by fatty carbon and carbonyl carbon. In addition, the contents of active groups (hydroxyl, carboxyl, and methyl/methylene) in lignite after bioretardation are lower than those in raw coal, and methyl/methylene content is decreased by 96.5%. The comparison shows that the flame-retardant performance of biological retardants is better than that of chemical retardants, which provides an effective solution for the efficient prevention and control of spontaneous combustion disasters in coal mines.

Keywords: mine fire prevention; lignite; spontaneous combustion of coal; retarding agent; microorganism

1. Introduction

China's coal mining sector is faced with complicated mining conditions and diversified coal species. Compared with other coals, lignite has the lowest degree of coalification and is characterized by high water content, highly volatile substances, and low carbon content. The ignition point of lignite is relatively low due to the high water content. In addition, when the internal water of lignite evaporates, the number of surface pores increases, the specific surface area of the coal increases, and internal temperatures increase rapidly. Highly volatile substances inside lignite are released when heated and mixed with oxygen to form flammable gas, while the low carbon content means that less ash and ash charcoal will be produced during the combustion of lignite, resulting in more heat being concentrated within the coal itself and thus accelerating the spontaneous combustion process. Therefore, lignite is prone to spontaneous ignition when exposed to air during mining, which is an important object of mine fire prevention and control. Globally, the spontaneous oxidation

combustion mechanisms of coal have been widely discussed by scholars. Among them, the theory of coal–oxygen recombination is a theory with great influence. By conducting repeated experiments, the adsorption effect of coal on oxygen has been confirmed. In order to further clarify the chemical mechanism of the coal–oxygen recombination theory, predecessors extended the free radical theory and revealed the transformation of organic compound molecules in coal during the oxidation process from a chemical perspective [1]. The spontaneous combustion of coal is a kind of self-accelerating chain exothermic reaction. Spontaneous combustion occurs when coal absorbs oxygen from the air. Oxygen reacts with hydrogen atoms in the active –CH group inside the coal to form a carbon-free radical, and it reacts with –COOH to decarboxylate it, thereby forming a peroxide. The decomposition of peroxides produces the hydroxyl and ether-oxygen radicals involved in chain reactions. The heat generated by this process gradually heats up the coal [2]. Coal generally proceeds through three stages: from spontaneous combustion to open flame. The first stage comprises a reaction with oxygen, a small amount of heat is released, and a weight equivalent to the mass of the adsorbed oxygen is added. This stage is called the incubation period of spontaneous coal combustion because there are no obvious external signs during the development of this stage. After the incubation period, with the continuous development of the oxidation process, newly generated carbon free radicals participate in the above-mentioned reaction, and the oxidation rate of activated coal molecules increases. With respect to the process of oxidation, there is an obvious thermal effect and dry distillation reaction. The evolution of active groups in lignite at low temperatures was studied via infrared technology and X-ray photoelectron spectroscopy. The results show that hydroxyl, adipose ethers, methylene, and methyl groups play an important role in the oxidation of lignite at low temperatures below 200 °C. Carbonyl and carboxyl groups are important intermediates. Therefore, the multi-step evolution mechanism of hydroxyl, adipose ethers, and alkane during the low-temperature oxidation of lignite can be inferred [3]. During the rapid heating stage of coal, small oxidizing molecules such as $-CH_3$ and $-CH_2$ in the aliphatic hydrocarbon side chain oxidize to produce various functional groups, carbon monoxide, carbon dioxide, methane, and other fire gases. At this stage, when the heat released by the coal body is greater than the heat released by the environment, the heat accumulates, and the temperature of the coal body continues to increase, which eventually leads to the spontaneous combustion of the coal body, entering the third stage: that is, the spontaneous combustion period of coal [4].

People have studied the law of spontaneous combustion by constantly exploring the relevant factors of spontaneous coal combustion. Based on the combustion theory, there are different perspectives on how to inhibit combustion, such as isolating the contact between the coal's surface and oxygen, reducing the temperature of coal so that it is lower than combustion temperatures, and improving the activation energy of coal oxidation reactions from the perspective of chemical technology. Based on various principles, such as the inhibition of spontaneous coal combustion reactions, technical measures—such as grouting, filling, pressure equalization, inhibition, and the use of inert gas, gel, and three-phase foam—are proposed to inhibit coal spontaneous combustion [5].

Among all kinds of existing fire prevention technologies, research on the use of inhibitors for fire prevention is still in the process of development [6–9]. Currently, commonly used inhibitors can be divided into the following: (1) Liquid film is formed on the surface of the coal seam via inhibition mechanisms, thereby preventing further contact reactions between coal molecules and oxygen in the air. (2) The blocking agent reacts with heat release, and the surrounding water is heated and vaporized to absorb heat, thereby preventing heat accumulation inside the coal seam. (3) The inhibitor reacts with the active groups in the macromolecular structure of coal to reduce the number of active groups, thereby preventing coal–oxygen reactions [10]. From the point of view of inhibition properties, the existing inhibitors can be divided into physical, chemical, and composite inhibitors. Physical inhibitors can effectively fix the water content in coal; reduce the possibility of spontaneous coal combustion; and prevent oxygen concentrations in coal composites,

mainly with respect to chlorine salts, halogen salt inhibitors, gel inhibitors, foam inhibitors, polymer inhibitors, etc. Compared to raw coal, the peak temperature and total heat release of the retarded inorganic salt coal sample decreased significantly, and the apparent activation energy increased significantly, thus effectively preventing the spontaneous combustion reaction of coal [11]. Predecessors analyzed the flame-retardant effect of inorganic salt retardants on different coal types by changing the types of coal and retardants. It was concluded that different inorganic salt inhibitors should be used for different coal types [12]. A large number of studies and practices [13–16] have shown that the physical mechanism by which inorganic salt inhibitors can inhibit coal spontaneous combustion comprises chloride aqueous solutions that contain metal ions, such as CaCl2 and MgCl2; these have strong hygroabsorbance. After being sprayed onto the coal's surface, water vapor in the air can be oxidized and adsorbed at low temperatures so that it adheres to the coal's surface. The adhesion isolates the direct contact between oxygen and the coal's surface, and the temperature of the coal body increases relative to oxidation during later stages; moreover, the water vapor in the solution evaporates, increasing the internal heat dissipation of the coal body.

Chemical inhibitors can directly interfere with the REDOX reaction in coal and interrupt the chain reaction by forming a stable structure with its active functional groups [17]. Inorganic salt aqueous solutions contain a certain proportion of calcium, magnesium salts, or compounds; these solutions not only have a flame-retardant effect on coal but also act as traditional chemical fire inhibitors. Commonly used examples include calcium chloride, magnesium chloride, calcium hydroxide, and water glass. From a macroscopic point of view, the treatment of coal samples with halogen retarders can significantly reduce the functional groups in the oxidation reaction, help prevent free radical reactions, and inhibit the oxidation reaction rate. In order to further clarify the oxidation inhibition process of inorganic salts from the perspective of microscopic molecular structure, the internal elemental composition of coal molecules is determined via a combination of industrial analysis, elemental analysis, and Fourier transform infrared spectroscopy; and nuclear magnetic resonance carbon spectrum test, X-ray diffraction, and other test and analysis methods. Furthermore, the occurrence of each element and the carbon content at different positions in the chemical structure of coal is determined, and the approximate derivation and modeling of the macromolecular structure of coal are finally realized; moreover, the chemical reaction process is simulated via software [18]. According to current research, the difficulty of exploring this problem and the focus of current research lies in the accurate construction of the molecular model of this complex polymer coal mixture. On this basis, predecessors have studied the structural changes in several inorganic salt inhibitors with respect to coal from the molecular point of view and evaluated their respective inhibition efficiency. For example, by studying the structural fragments of coal molecules, it is proposed that metal ions can form coordination bonds with atoms in some active groups, thereby reducing the activity of reactive groups in coal and oxygen reactions. A systematic study has been conducted on the N-containing active groups in coal, and the results show that calcium ions react with N-containing active groups in coal structure to form stable complexes, improve the active structure of coal, and greatly improve the stability and antioxidant capacity of coal [19]. Via thermal analysis, infrared spectroscopy, oxidation analysis, and other experimental tests, it has been proven that phosphate and $MgCl_2$, as synergistic inhibitors for inhibiting spontaneous coal combustion, can effectively reduce heat during the process of spontaneous coal combustion and reduce functional groups such as –OH and $–CH_2$ in treated samples [20]. According to the oxidation temperature experiment and Fourier infrared spectral analysis, it is observed that the sodium persulfate treatment of coal samples can increase the amount of stable ethers, alkyls, and carboxylic acids in the molecular structure, thus significantly improving the flame retardant's performance [21]. From a technical perspective, in order to effectively solve the limitations and deficiencies of a single type of chemical retarder, some predecessors proposed combining it with different types of retarders to form a composite retarder that is, in turn, used to

inhibit spontaneous combustion of coal. Examples include carbon/oxygen free radical trapping agents and a magnesium chloride complex [22]; foam carrier combined with thermoplastic and coal powder [23]; sodium polyacrylate–anthocyanin complex inhibitor; and the use of temperature-sensitive smart gel tea polyphenol coatings [24]. In order to reduce the loss of chemical reagents and extend the short-term resistance of traditional chemical inhibitors, microcapsule encapsulation with respect to chemical reagents can improve the stability of traditional chemical reagents and provide convenience for injection into coal seams. The principle is to inject the microcapsule inhibitor into the coal seam in advance when the coal body is not oxidized [25]. When the oxidation of the coal seam reaches a certain temperature point, the chemical inhibitor wrapped in the microcapsule begins the process of inhibition. Currently, the microcapsule coated with tea polyphenol inhibitors and ethylenediamine tetraacetic acid coated with polyethylene glycol 20000 and pentaerythritol stearate exhibit significant chemical inhibition effects and can improve the activation energy of the reaction [26].

Currently, the application of MICP technology in environmental protection and dust control is relatively mature, and its calcium carbonate product significantly changes its physical and chemical properties by modifying materials, which can effectively realize the solidification effect on soil. In terms of strengthening concrete strength, free calcium ions in carbonic acid ion concrete generated by urease hydrolysis react to form solid calcium carbonate deposits, fill cracks in concrete, and improve the strength and durability of concrete. In some construction sites, calcium carbonate can be combined with particles in the soil to form a stable structure, reduce the flying and diffusion of dust, improve the construction environment, and protect the health of workers. In addition, calcium carbonate can also be used to control soil erosion, increase the cohesion and stability of soil, reduce soil erosion, and protect soil resources [27]. Given this characteristic, this paper proposes a new method and principle for inhibiting the spontaneous combustion of lignite by inducing calcium deposition via microorganisms. A series of controlled experiments are carried out to determine the optimal culture environment for microorganisms, and four coal samples—raw coal, bioinhibited coal, chemically inhibited coal, and water-immersed coal—are prepared. SEM, pore size analysis, and FT-IR tests were carried out to study the changes in surface morphology, pore structure, active functional groups, and other microscopic characteristics of the four lignite samples before and after inhibition; analyze the inhibition mechanism and change rule; and reveal the inhibition mechanism of microbial inhibitors on spontaneous lignite combustion from the perspective of microstructure. In the coal sample after biological inhibition treatment in the experiment, the inorganic salt is attached to the surface of the coal body, and this will not pollute the environment with the loss of groundwater or solution and is more environmentally friendly and efficient than traditional chemical inhibition agents.

2. Experimental Material

2.1. Preparation of Biological Inhibitors

The Bacillus pasteurelli used in the experiment was purchased from Beijing Beina Biotechnology Co, Ltd., Beijing, China (strain number ATCC11859). The urease produced by this strain can decompose urea in two stages to obtain ammonia and carbonic acid. With the addition of a calcium source, carbonate ions in the solution combine with calcium ions to form calcium carbonate with strong cementing abilities [28]. Applying microorganisms to inhibit the spontaneous combustion of coal mainly comprises using the produced calcium carbonate to block the pores of coal; this significantly reduces the specific surface area of coal, reducing oxygen contact with respect to the coal's surface. The growth of Bacillus pasteurii is mainly affected by temperature and pH, and it has strong adaptability to the environment and can survive in environments with high acid, alkali, and salt concentrations. Studies have shown that the optimal growth temperature of this bacterium is 30 °C in a more alkaline environment [29], and the optimal cultivation conditions, such as pH and cultivation time, are determined via further controlled experiments.

According to the results of the control experiment, the strains were cultured in a weak alkaline environment with a PH of 7.5 for 48 h, and the number of microorganisms and urease activity in the culture medium was the highest. When calcium chloride was selected as the calcium source, the concentration of cementing fluid was 1 M, the ratio of cementing fluid to bacterial fluid was 1:1, and the ratio of urea to calcium chloride was 1:1.5; moreover, the quality of calcium carbonate was the highest. The influence of culture conditions on biological bacteria solution is shown in Figure 1.
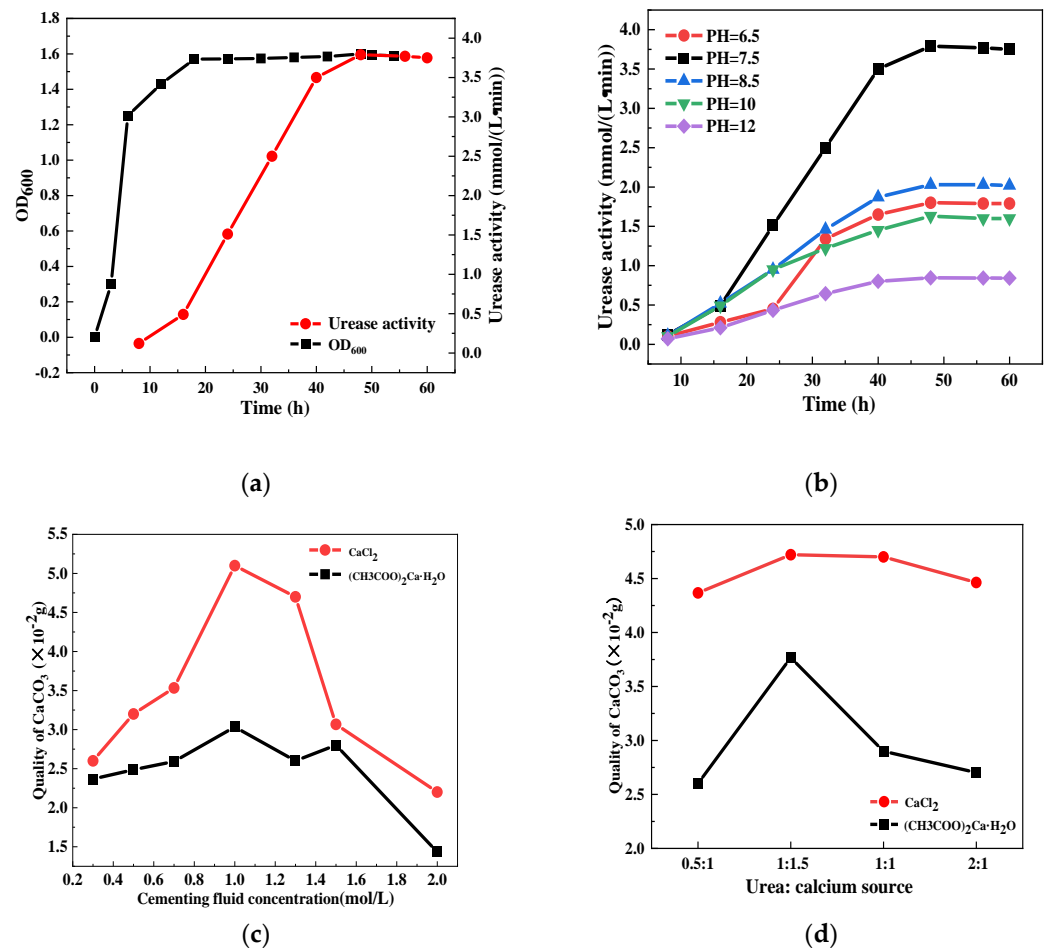

(**a**)

(**b**)

(**c**)

(**d**)

Figure 1. Influence of changing culture conditions on bacterial activity. (**a**) The change in microbial concentration and urease activity relative to culture time. (**b**) The changing trend of urease activity relative to time in different pH environments. (**c**) The calcium carbonate quality produced by the two calcium sources in the culture medium with different cementing fluid concentrations. (**d**) shows the calcium carbonate deposition produced by the two calcium sources at different ratios of cementing fluid to bacterial fluid.

2.2. Preparation of the Experimental Coal Sample

The object of this experiment was lignite, which was accurately tested and analyzed according to the standard experimental coal sample method [19]. Fresh coal samples were taken from the site and sealed and stored. After crushing treatments in the laboratory, samples with particle sizes of 40~80 mesh and 200~300 mesh were selected and dried for 48 h under a vacuum environment for subsequent use. Four groups of lignite coal powder with a mass of 5 g were weighed, and one group of coal samples comprised raw coal samples without treatment; this group was placed in a 40° drying oven for 48 h under vacuum drying. The remaining three groups underwent the following procedure: 10 mL of the immersed coal sample that was dried after 24 h of distillation soaking in water was added, and a 1 mol/L calcium chloride solution and 5 mL of 1 mol/L sodium bicarbonate

solution were added so that the coal sample could react within the completely immersed state for 24 h; then, the chemically inhibited coal sample was dried. In addition, 5 mL of calcium chloride solution with a concentration of 1 mol/L and 5 mL of microbial culture medium that was cultured for 48 h (bacterial activity OD600 = 1.6) were added to the bioinhibited coal samples, which were dried after a 24 h reaction in a completely immersed state. The drying method of each sample was the same as that of the raw coal sample. Four differently treated experimental sample groups were obtained after each sealing, and the same standard was used to prepare the experimental long-flame coal sample. The prepared experimental coal samples are shown in Figure 2.
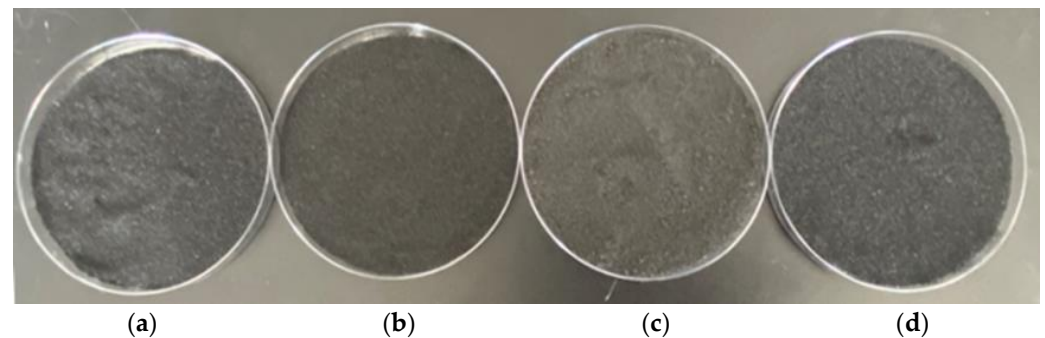

| (a) | (b) | (c) | (d) |

Figure 2. Sample drawing of experimental coal. Lignite samples from left to right: (**a**) raw coal, (**b**) immersion coal, (**c**) chemically inhibited coal, and (**d**) biologically inhibited lignite.

The content of C, H, N, and S in lignite can be determined via industrial analysis and elemental analysis, while the content of O can be calculated via subtraction. Test results are shown in Table 1.

Table 1. Lignite industry analysis and elemental analysis table. M_{ad} stands for air-drying-based moisture, A_{ad} stands for ash, V_{ad} stands for volatiles, and FC_{ad} stands for air-drying-based fixed carbon.

Sample	M_{ad} (%)	A_{ad} (%)	V_{ad} (%)	FC_{ad} (%)	C (%)	H (%)	O (%)	N (%)	S (%)
Lignite	0.86	6.81	23.15	69.18	65.00	4.54	29.19	0.93	0.34

3. Experimental Methods

3.1. Electron Microscope Experiment of Retarded Lignite

The four coal sample groups were dehydrated and sprayed with gold to ensure good electrical characteristics. A Quanta^{TM}250 scanning electron microscope was used to observe and analyze their surface structural characteristics.

3.2. Low-Temperature Nitrogen Adsorption Experiment

Each group contained approximately 2.5 g of lignite, and the long-flame coal samples were weighed in a sample tube for the 10 h degassing treatment. The empty tube mass, M1, of the sample tube and the sample tube mass, M2, of the coal sample with degassing and water removal in the pores were weighed before and after degassing. After that, the rapid automatic specific surface area NOVA touch and aperture analyzers were used to perform low-temperature nitrogen adsorption experiments on coal samples at ambient temperatures above 77 K and within a relative pressure range of 0.008~0.98. The measurement principle is to use nitrogen as the measuring medium and take advantage of the adsorption characteristics of coal to measure the specific surface area, total pore volume, and average pore size of the sample [30]. After measurements, the BET equation was used to determine the nitrogen monolayer saturation adsorption capacity in order to estimate the specific surface area of the experimental coal sample [31]. The BJH method was used to analyze pore size distributions [32], and the capillary condensation theory and equivalent exchange

principle were used to measure the volume of liquid nitrogen in the pore and then estimate the pore size; then, the total pore volume and average pore size of the coal sample can be calculated via formulas.

3.2.1. Calculation of the Specific Surface Area

By applying the BET equation, the specific surface area of each layer on the isothermal adsorption line can be calculated, and the interaction between the single-layer adsorption amount, V_m, and the multi-layer adsorption amount, V_m, can be deduced [33]:

$$P/(V(P_0 - P)) = 1/(V_m \times C) + (C - 1)/(V_m \times C) \times P/P_0 \tag{1}$$

P: partial pressure of nitrogen, Pa;
P0: saturated vapor pressure of nitrogen at adsorption temperatures, Pa;
V: the actual adsorption amount of nitrogen on the sample's surface, cm^2/g;
V_m: nitrogen monolayer saturation adsorption capacity, cm^2/g;

$$V_m = 1/(A + B) \tag{2}$$

D: constant related to the adsorption capacity of the sample;

$$D = 1 + (A \times B) \tag{3}$$

S_g: specific surface area, m^2/g.

$$S_g = 4.325 \times V_m \tag{4}$$

Using the BET equation, P/P_0 as the x-axis, and $(P/P_0)/(V(1 - P/P_0))$ as the *y*-axis, a linear equation of the form y = Ax + B can be obtained; then, V_m can be determined by combining the calculated results with slope A and intercept B.

3.2.2. Calculation of the Aperture Distribution

The coal pore size division method proposed by IUPAC has currently become the most commonly used method, and it divides the pores of coal into three categories according to the changes in the pore size of the coal and the influence of solid substances—micropores (<2 nm), mesoporous (2~50 nm), and macroporous (>50 nm)—in order to better meet the needs of different applications. Currently, BJH has become the most widely used and mature calculation model of aperture distributions; it is based on the Kelvin capillary condensation theory and is widely used in a variety of theories. In this paper, the BJH method is used to analyze the pore size distribution, where dv (r) represents the differential relationship between pore volume and pore size, reflecting the function of pore density distributions: the proportion of pore volume. The cumulative pore volume refers to the cumulative volume of coal samples with respect to an increase in pore volume.

Using capillary condensation theory and the equivalent exchange principle, the volume of liquid nitrogen in the hole can be accurately measured using adsorption technology; then, the size of the hole can be accurately estimated. The following formula can be used to calculate the total pore volume and average pore diameter:

$$\ln(P/P_0) = 2\gamma\overline{V}/rT \tag{5}$$

where *r* is the pore range, nm; γ is liquid nitrogen surface tension, N/m; *T* is the absolute temperature, K; R is the universal constant of gas, 8.314 $J \cdot mol^{-1} \cdot K^{-1}$; *V* is the adsorption angle; and liquid nitrogen adsorption is set at r = 0.

The aperture size's calculation formula is as follows:

$$\overline{d} = 4V/A \tag{6}$$

where *V* is the total pore volume of the adsorbent, mL; and *d* is the average aperture, nm.

3.3. NMR and FTIR Tests

3.3.1. Nuclear Magnetic Resonance Carbon Spectrum Test

Nuclear magnetic resonance analyses of lignite were performed using ^{13}C-NMR technology. Using a solid double resonance probe with an outer diameter of 6 mm ZrO_2, its speed was 7 KHz, resonance frequency was 75.43 MHz, sampling time was 0.05 s, pulse width was 4.2 μs, cycle delay time was 4 s, hydrocarbon cross-polarization time was 3 ms, and scanning times were between 2000 and 3000 times. Because of the different chemical components of coal carbonization, their chemical shifts produce multiple resonance absorption peaks, which renders ^{13}C-NMR analysis very difficult. Therefore, in this study, Origin2019 was used to perform peak sub-peak fitting for the NMR spectra. When the R^2 variance of the fitted curve and the actual curve approaches 1, the fitting results are more accurate and reliable.

3.3.2. Fourier Infrared Spectroscopy Experiment

A Bruker VERTEX 80v infrared spectrometer was used in the experiment. According to the relevant regulations [21], the experimental environment was clean and free of strong electromagnetic field interference sources, and the coal sample was preheated for 30 min. Eight types of experimental lignite and long-flame coal samples were tested according to the standard experimental measurement process. A 1 g sample of solid coal powder with particle sizes between 200 and 300 mesh was prepared. The test sample was made by mixing KBr with the coal sample and pressing it. The scanning range was between 4000 and 400 cm^{-1}, and 64 sample scans were completed.

4. Results

4.1. Scanning Electron Microscope Analysis of Lignite's Surface Structure

The SEM images of the four groups of samples are shown in Figure 3.

From top to bottom, the images are (a) raw coal samples, (b) water-immersed coal samples, (c) chemically inhibited coal samples, and (d) biologically inhibited coal samples, respectively. Via observations, it is observed that in the figure, there are a large number of pores that were formed via gas generation and gas accumulation due to low metamorphism in the process of coal production, and exogenous pores were formed via geological structures after the consolidation of diagenesis in some solution pores. These are secondary pores formed via the dissolution of soluble minerals in coal after long-term immersion in water. Under an electron microscope, there is almost no difference in surface structure between lignite treated with water and raw lignite coal.

Under an electron microscope, the surface structure of the coal sample (c) and coal sample (d) treated with chemical and biological inhibitors is significantly different from that of raw coal with respect to morphology. This is because the solid calcium carbonate product on the surface of the coal sample—produced via the two inhibition methods—results in a more dense and compact coal sample surface after treatment compared to the raw coal sample and water-immersed coal sample. By enlarging coal samples (c) and (d), it is observed that the calcium carbonate produced via the chemical inhibition treatment and covered on the surface of the coal sample mainly exhibits a massive distribution, while the calcium carbonate produced via the biological inhibition treatment presents a more dense spherical distribution. The main reason for this phenomenon is that the biological inhibition process uses microorganisms as the intermediate medium. The resulting calcium carbonate combined with the viscosity of microorganisms themselves can more firmly seal the pores generated by various factors in the coal seam, significantly reducing the contact area between the coal surface and oxygen.
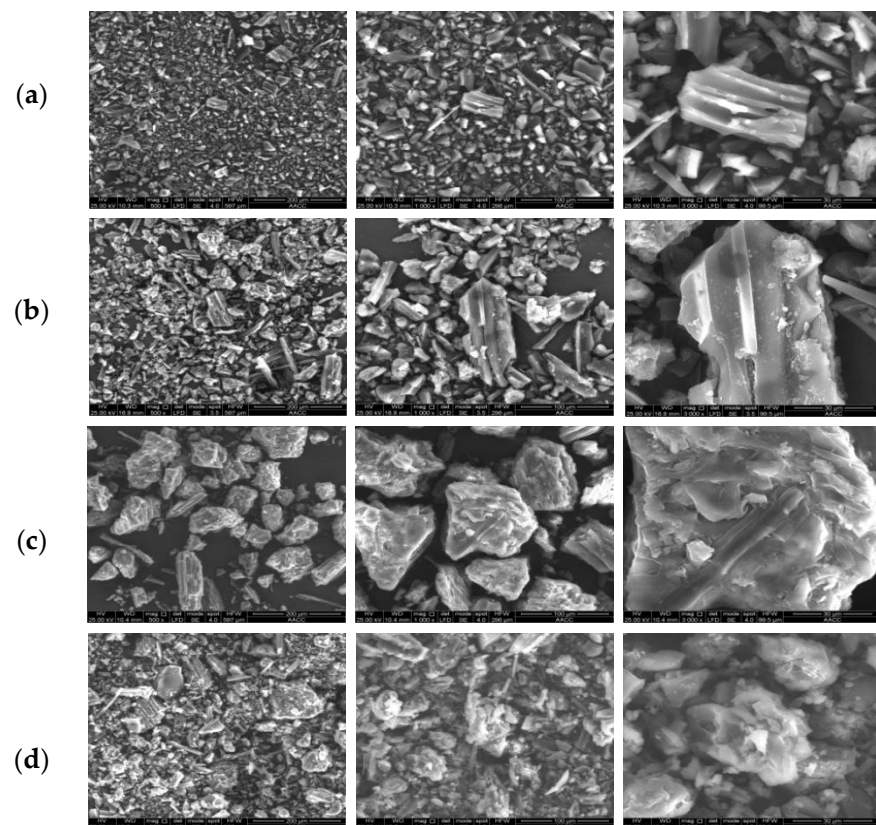
Figure 3. Lignite scanning electron microscopy: (**a**) raw coal; (**b**) immersed coal; (**c**) chemically inhibited coal sample; (**d**) biologically inhibited coal sample. Enlarged 500×, 1000×, and 3000× images of each group of experimental lignite samples from left to right.

4.2. Experimental Analysis of the Inhibited Lignite's Pore Size

4.2.1. Aperture Distribution Characteristics

The pore size distributions of the four lignite samples and four long-flame coal samples treated with different inhibitors are shown in Figure 4a,b, respectively. In the figure, the horizontal coordinate represents the pore's size, and the vertical coordinate represents the number of holes. It is observed in (a) that most internal pores of raw lignite coal are medium and large pores, and a few are micropores. Compared with raw coal, the pore size of lignite treated with water immersion increased slightly, and the changing trend was consistent with that of raw coal. However, the number of macropores and mesoporous pores in the lignite samples after bioresistance treatment was greatly changed, and the number of macropores above 50 nm was significantly reduced compared with that of raw coal, while the number of micropores exhibited little change. It is observed in (b) that most long-flame coals are micropores and mesoporous pores with relatively small pore sizes, and large pores are few in number. These phenomena verify that Bacillus pasteurelli lives well in macropores and produces high urease activity. It was observed that the total number of pores in the bioinhibited coal sample is significantly lower than that in the chemically inhibited coal sample, and this is observed by comparing the number of pores in each bioinhibited coal sample. The obvious change in the number of holes indicates that the effect of biological inhibition is better than that of chemical inhibition with respect to the sealing of internal holes in coal samples.
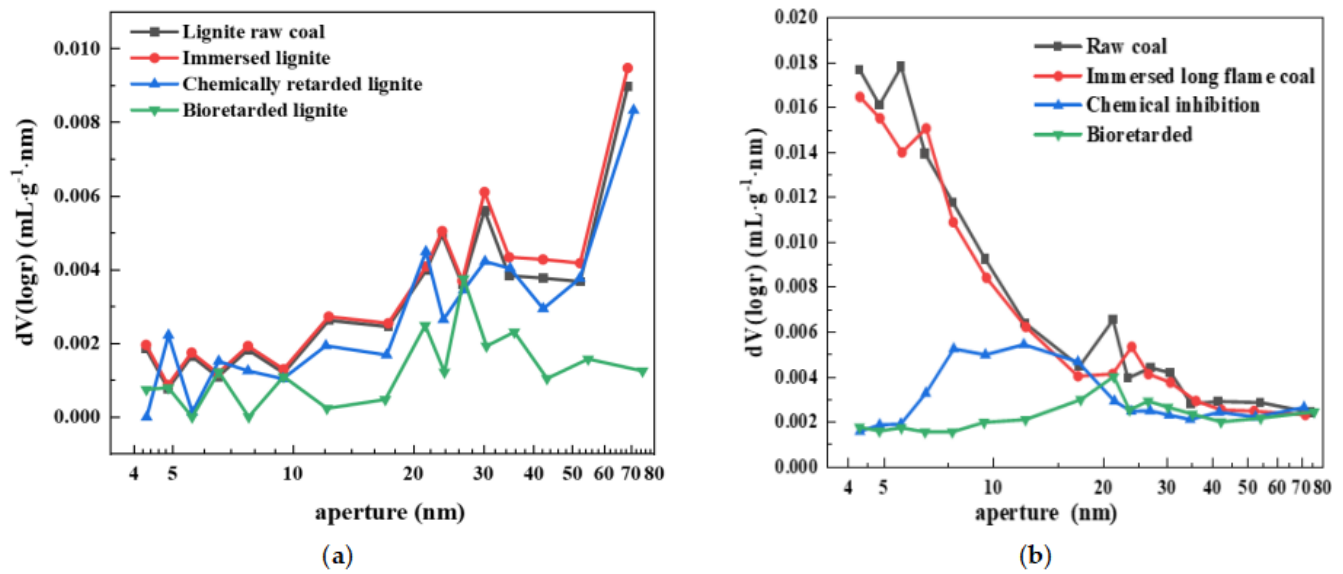
Figure 4. Pore size distribution diagram. (**a**) Pore size distribution of lignite. (**b**) Pore size distribution of long-flame coal.

4.2.2. Pore Structure Characteristic Parameter Analysis

The multilayer physical adsorption model of the BET theory can effectively capture adsorption characteristics within the range of 0.05~0.35, but when the range exceeds 0.05, the formation of multilayer physical adsorption is affected by capillary condensation, thus making the surface's non-uniformity more obvious [34]. Therefore, within this range, the BET theory can capture the adsorption characteristics more accurately. In this paper, the BET equation is used to calculate the specific surface area, and the relative pressure (P/P_0) is set between 0.05 and 0.35.

According to IUPAC, the coal's pore size is divided into three types—micropores, mesopores, and macropores—in order to better meet different application requirements. The BJH pore size distribution calculation model is developed from the Kelvin capillary condensation theory [35]. The adsorption properties of nitrogen in samples were studied via the BJH method, and the pore size distribution was analyzed in detail. In Table 2, the total pore volume P_V and the pore's specific surface area P_S of the four experimental coal samples are calculated using the above method. Two parameters, D_{pv} and D_{ps}, are introduced to represent the different percentages of P_V and P_S relative to the experimental coal samples compared with raw lignite coal samples, respectively. The positive and negative values of the two parameters, respectively, reflect an increase or decrease in the total pore volume and specific surface area of the coal sample after inhibition treatment. Positive values mean that the value of the treated coal sample increases compared with the raw coal, while negative values mean that the value of the corresponding coal sample decreases compared with the raw coal.

$$D_{Pv} = \frac{P_{vi} - P_{v1}}{P_{v1}} \times 100\% \qquad (7)$$

$$D_{Pv} = \frac{P_{vi} - P_{v1}}{P_{v1}} \times 100\% \qquad (8)$$

The pore structure of coal is closely related to the spontaneous combustion process. Via the coal spontaneous ignition simulation system, predecessors conducted temperature oxidation simulation tests on a variety of coal samples to explore the relationship between spontaneous coal combustion tendencies and the specific surface area of microscopic pore structure and pore size [36]. The results show that the coal sample with smaller specific surface areas exhibited higher oxidation temperatures. Therefore, the coal pore's specific

surface area can be effectively reduced by blocking the primary pores inside the coal, and the spontaneous combustion of coal can be inhibited by preventing the contact reaction between oxygen and the coal's surface. MICP is a form of bioinduced mineralization that widely exists in nature, and its macroscopic process comprises the production of carbon dioxide via microbial metabolism in an alkaline environment containing free calcium ions and the formation of calcium carbonate deposits. Bacillus uses urease to hydrolyze urea in order to produce a large number of carbonate ions in the environment. Extracellular polymeric substances (EPSs) produced via the metabolism of some microorganisms usually contain hydroxyl, amide, amine, carboxyl, and other negative ionic groups, resulting in electronegative extracellular polymeric substances. When there is a certain amount of Ca^+ in the environment around the cell, the Ca^+ in the environment is continuously adsorbed on the surface of electronegative cell membranes, and they finally combine with CO_3^{2+} to generate $CaCO_3$ precipitation. These products will adhere to the surface of the coal seam, sealing the surface pores of the coal seam and reducing the contact area between coal and oxygen. From the analysis shown in Table 2, it is observed that the total pore volume P_V and specific surface area P_S of the coal sample treated with the two inhibitors are significantly reduced compared with the raw coal sample, and the D_{pv} and D_{ps} of the bioinhibited sample are both lower than those of the chemically inhibited sample. This is because the adhesion of calcium carbonate induced by Bacillus pasteurelli is higher than that of ordinary calcium carbonate, which can result in improved adhesion between coal particles and sealed coal seams. Therefore, both inhibitors can effectively plug the pores in coal, and it is observed that the effect of biological inhibition using Bacillus pasteuris is more obvious than that of chemical inhibition.

Table 2. Specific surface area and total pore volume determination results of coal samples.

Coal Sample		P_V (mL/g)	D_{pv}	P_s (m²/g)	D_{ps}
Lignite	Raw coal	0.00476	-	1.340	-
	Bioretarded	0.00150	−68.49%	0.348	−74.03%
	Chemically inhibited	0.00258	−45.79%	1.004	−25.07%
	Immersed	0.00479	0.63%	1.335	−0.37%
Long-flame coal	Raw coal	0.009637	-	3.051	-
	Bioretarded	0.0033540	−65.19	0.952	−68.79
	Chemically inhibited	0.0047644	−50.56	1.185	−61.16
	Immersed	0.008547	−11.31	2.032	−33.39

4.3. Nuclear Magnetic Resonance Carbon Spectrum Characteristics and Infrared Spectrum Experimental Analysis

4.3.1. ^{13}C-NMR Characteristic Analysis

The nuclear magnetic resonance detection of coal samples can effectively determine the structure information of organic matter [37], and nuclear magnetic resonance technology is used to detect lignite coal samples. Based on the analysis of detection results, we observed five distinct carbon signals in the lignite, which can be fitted via the Origin2019 software to better understand the structural characteristics of lignite.

Figure 5 shows the fitting diagram of ^{13}C-NMR. According to the structural attribution of chemical shifts in the ^{13}C-NMR diagram [38], the functional group belonging to the region where each absorption peak appears is determined. According to the image, the chemical shift of this sample is mainly concentrated within 0~90 ppm relative to aliphatic carbon, 100~170 ppm relative to aromatic carbon, and 160~250 ppm relative to carbonyl carbon. By fitting the image, we can observe that the aromatic carbon region exhibits the highest resonance absorption peak, followed by the fatty carbon region, and the carbonyl carbon region exhibits the lowest absorption peak. This shows that the chemical structure of the coal sample is mainly composed of aromatic carbon, followed by fatty carbon and carbonyl carbon.
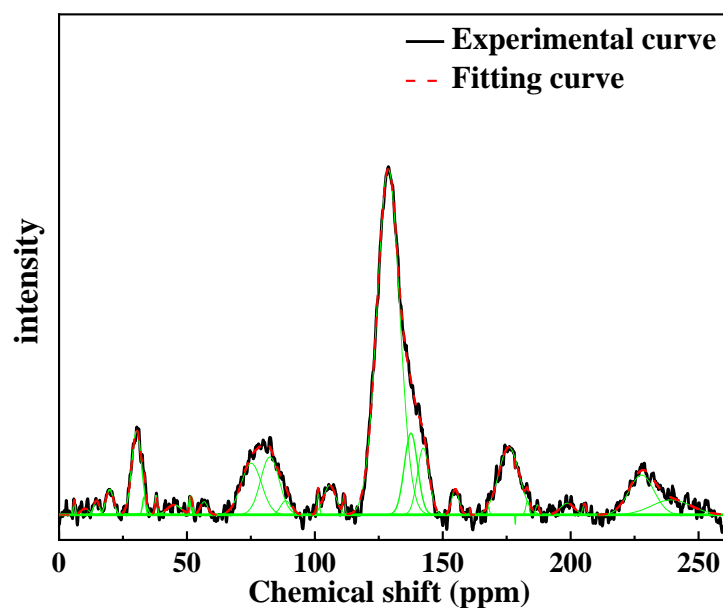
Figure 5. The ^{13}C-NMR detection of the peak fitting spectrum. The green lines represent the peak fitting results.

According to the theory of coal–oxygen recombination, the spontaneous combustion of coal is a result of heat accumulation generated by the reaction between the active groups and oxygen in coal molecules, which increases the temperature of the coal seam, reaching the combustion point. This process can be divided into different stages, including the low-temperature oxidation stage, high-temperature oxidation stage, and combustion stage.

During coal oxidation reactions, the time period and the conditions of coal's internal carbon structures are affected by the internal temperature of coal, oxygen concentrations, and other factors. Among them, fatty and carbonyl carbon can oxidize during the low-temperature oxidation stage if there is sufficient oxygen and accumulate heat for further reactions. Aromatic carbon usually comprises aromatic rings. Aromatic carbon is relatively stable in the oxidation reaction of coal, which requires high temperatures and oxygen concentrations [39]. Therefore, aromatic carbon usually participates in the oxidation reaction of coal only when heat accumulates at higher temperatures.

4.3.2. Infrared Spectrum Analysis of Coal Samples before and after Inhibition

During spontaneous coal combustion processes, internal molecular active groups play an important role during different stages of spontaneous combustion. In the low-temperature oxidation stage, the active groups in coal, such as hydroxyl (–OH), aldehyde (–CHO), and carboxylic (–COOH), can react with oxygen at normal temperatures to generate heat and carbon dioxide, providing reaction power for the further oxidation of coal. With the continuous accumulation of heat, methyl–methyl (CH3–CH2–) in the structure of coal aromatics and aliphatic hydrocarbons participates in the cracking reaction, producing volatile substances and free radicals. These volatile substances and free radicals may participate in oxidation reactions and further accelerate the spontaneous coal combustion process. Therefore, if the reduction in the reactive activity of the active group is observed after the application of the inhibitor, the inhibitor can reduce the spontaneous combustion tendency of coal.

The addition of biological inhibitors prevents the natural microstructure of coal by reducing the number of active groups to reduce the reaction rate. Combined with the infrared spectrum of coal samples, the main functional groups in coal can be divided into four categories: hydroxyl, oxygen-containing functional groups, aliphatic hydrocarbons, and aromatic hydrocarbons [40]. In this paper, content variations are analyzed by comparing

the size of the peak area of the functional group. The peak attribution table of the main spectral features is shown in Table 3.

Table 3. Peak attribution table of the main spectral characteristics.

Peak Type	Peak Number	Peak Position	Functional Group	Peak Attribution
Oxygen-containing functional groups	1	3697~3590	–OH	Free hydroxyl group
	2	3500~3200		An intermolecular hydrogen bond between a phenol hydroxyl group, an alcohol hydroxyl group, and an amino group
	3	1790~1715	C=O	Stretching vibration of the carbonyl group
	4	1715~1690	–COOH	Carboxyl group
	5	1275~1010	C–O–C	Ether bond
Aliphatic hydrocarbon	6	2975~2950	–CH3	Methyl group with asymmetric stretching vibration
	7	1470~1430		Methyl with shear vibration
	8	1380~1370		
	9	2940~2915	–CH2	Methylene with asymmetric stretching vibration
	10	2870~2845		Methylene with symmetric stretching vibration
Aromatic hydrocarbon	11	3090~3030	–CH	Aromatic CH with stretching vibration
	12	1620~1490	C=C	C=C with stretching vibration in the aromatic ring
	13	900~700	——	Out-of-plane bending vibration of polyhedron-substituted aromatics

(1) Aromatic hydrocarbons

The aromatic structure is the core structure of coal molecules; only when the temperature is high will the molecular skeleton structure break. It was observed that there was no significant change in the aromatic substitution structure spectrum peak between the treated coal sample and the raw coal sample, indicating that the molecular skeleton structure of the coal was not changed after the biological inhibition treatment.

After analyzing the Fourier infrared spectrum of the coal samples inhibited at normal temperatures, it is observed that the active groups of the coal samples inhibited at normal temperatures are reduced, and the content of stable ether bonds is increased. In the low-temperature oxidation stage, the oxidation of formed ether bonds requires increased energy compared to the carboxyl groups, carbonyl groups, and hydroxyl groups. After adding microbial inhibitors at normal temperatures, the active groups of coal molecules underwent etherization reactions. In this manner, heat does not easily accumulate in the low-temperature oxidation stage, and the calcium carbonate produced later wraps around the coal and blocks the contact area between the coal and oxygen, slowing the reaction rate. These two aspects ultimately prevent the easy accumulation of heat in coal–oxygen reactions, and a longer reaction time is required to reach the burning point of the coal body, thus inhibiting the spontaneous combustion of coal. The energy change observed during the etherification reaction of the active groups of coal molecules under the condition of microbial inhibitors determines the difficulty of the reaction, which is manifested as the efficacy of biological inhibitors on spontaneous coal combustion.

(2) Fatty hydrocarbons

The distribution trend of aliphatic hydrocarbon characteristic peaks in coal samples is roughly the same. Methyl and methylene are one of the main reactive groups in the macromolecular structure of coal. The peak area of methyl and methylene in the coal sample after bioretarding treatment is significantly lower than that of raw coal, indicating that methyl and methylene in the molecular structure of coal can be consumed after bioretarding treatment, the number of active groups participating in the cracking reaction

can be reduced, and the generation rate of free radicals and volatile gases can be reduced in order to prevent the effects of spontaneous coal combustion.

(3) Hydroxyl group

Hydroxyl groups in coal are the main components of hydrogen bonds, and their type and strength affect spontaneous coal combustion risks. According to 3–7, within this characteristic hydroxyl peak band, the distribution and intensity of the characteristic peaks of experimental coal samples differ greatly. Hydroxyl's characteristic peak strength in coal samples after inhibition treatment is lower than that of raw coal, and the types of hydroxyl groups are also different. The number of intermolecular hydrogen bonds in the coal samples increases, while the number of intermolecular hydrogen bonds in the amino groups decreases. Moreover, the effect of biological resistance treatment is more obvious than that of chemical resistance treatments.

(4) Functional groups that contain oxygen

The oxygen-containing functional groups in coal mainly comprise carbonyl, carboxyl, and ether bonds. The carboxyl and carbonyl groups in oxygen-containing functional groups can combine with oxygen to produce more active small molecules in order to participate in the coal–oxygen reaction. Therefore, the higher the content of carboxyl and carbonyl groups in oxygen-containing functional groups, the more likely the coal–oxygen reaction will occur. With respect to the comparison of activity spectrum peaks in Figure 5, it is observed that the area and quantity of the carboxyl group's spectrum peaks with respect to coal samples that underwent bioinhibited treatment are reduced, and the reduction is greater than that of the coal samples that underwent chemical bioinhibition treatment. The results show that bioinhibition can reduce the active sites of oxygen-containing functional groups in coal structures and delay the reaction rate.

Microbial decomposition produces carbonate ions, and calcium ions are provided by calcium chloride, which etherifies the active functional groups of coal molecules in the calcium carbonate environment. After analyzing the Fourier infrared spectrum of coal samples inhibited at normal temperatures (Table 3 and Figures 6 and 7), it is observed that the active groups of coal samples inhibited at normal temperatures are reduced, and the content of stable ether bonds is increased. In the low-temperature oxidation stage, the oxidation of formed ether bonds requires increased energy compared to the carboxyl groups, carbonyl groups, and hydroxyl groups. After adding microbial inhibitors at normal temperatures, the active groups of coal molecules experience etherization reactions. In this manner, heat does not easily accumulate in the low-temperature oxidation stage, and calcium carbonate produced later will wrap around the coal and block the contact area between coal and oxygen, slowing down the reaction rate. These two aspects ultimately prevent the easy accumulation of heat during the coal–oxygen reaction, and a longer reaction time is required to reach the burning point of the coal body, thus inhibiting spontaneous coal combustion. The energy change in the etherification reaction of the active groups of coal molecules under the condition of microbial inhibitors determines the difficulty of the reaction, which is manifested as the efficacy of biological inhibitors relative to spontaneous coal combustion.

4.3.3. Analysis of the Spectral Peak Characteristics of Functional Groups

The main causes of spontaneous coal combustion are aliphatic hydrocarbons, hydroxyl groups, and functional oxide groups. By using Origin software, infrared spectral data are fitted from peak to peak to determine the number and proportion of different types of functional groups. The functional group changes in coal samples after different experimental treatments were accurately detected via sectional fitting. The absorption bands of hydroxyl, aliphatic, oxygen-containing functional groups, and aromatic hydrocarbons were $3600 \sim 3000$ cm^{-1}, $3000 \sim 2800$ cm^{-1}, $1780 \sim 900$ cm^{-1}, and $900 \sim 650$ cm^{-1}, respectively. Understanding these common functional groups is helpful for better understanding the changes in functional groups after coal treatment. The following parameters are intro-

duced to characterize the change in the content of different active groups in coals after resistance treatment.
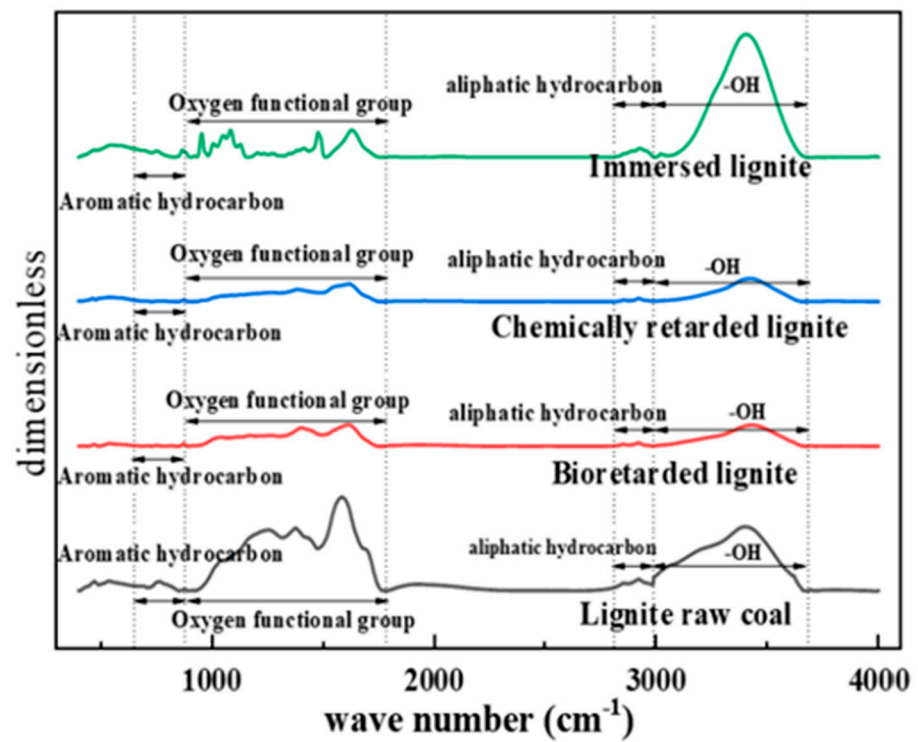
(a)
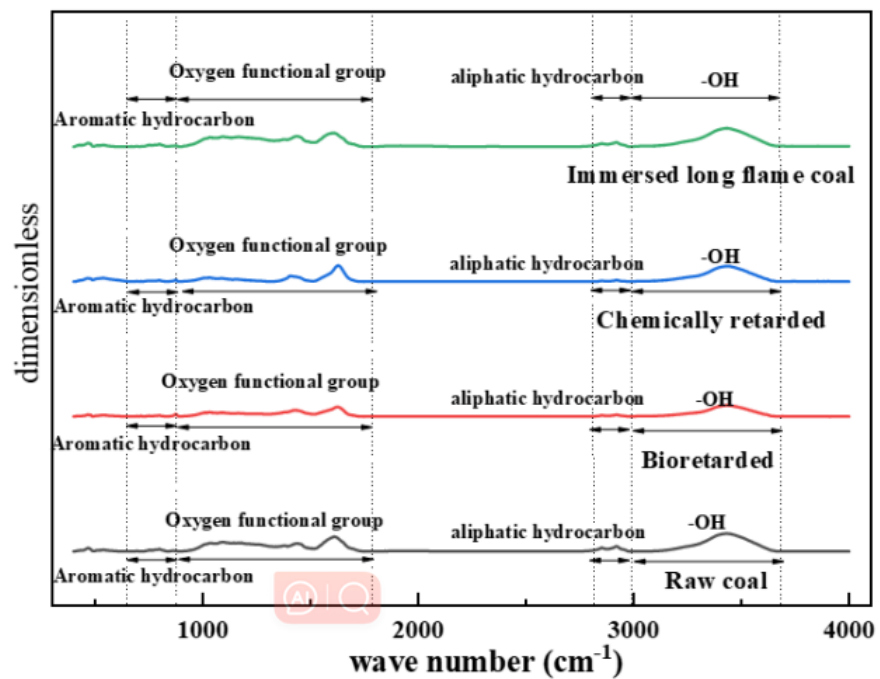
(b)

Figure 6. Infrared spectral curve: (**a**) lignite and (**b**) long-flame coal.

$$D_{-\mathrm{CH_3/-CH_2}} = \frac{EC_{-\mathrm{CH_3/-CH_2}} - RC_{-\mathrm{CH_3/-CH_2}}}{RC_{-\mathrm{CH_3/-CH_2}}} \times 100\% \tag{9}$$

$$D_{-\mathrm{OH}} = \frac{EC_{-\mathrm{OH}} - RC_{-\mathrm{OH}}}{RC_{-\mathrm{OH}}} \times 100\% \tag{10}$$

$$D_{-\mathrm{COOH}} = \frac{EC_{-\mathrm{COOH}} - RC_{-\mathrm{COOH}}}{RC_{-\mathrm{COOH}}} \times 100\% \tag{11}$$

In the formula, EC represents the content of the corresponding active groups in coal samples that were treated with different methods; RC represents the initial content of the corresponding functional groups in raw coal; $D_{-\mathrm{CH3/-CH2}}$, $D_{-\mathrm{OH}}$, and $D_{-\mathrm{COOH}}$, respectively, represent changes in the content of methyl/methylene, hydroxyl, and oxygen-containing functional groups (carboxyl groups) in treated coal samples compared to raw coal. The detection shows that the hydroxyl content of the coal sample after resistance treatment is reduced, indicating that the two treatment methods combine the hydroxyl groups within the coal structure, reducing the chance of contact between the hydroxyl group and oxygen. Methyl and methylene groups in aliphatic hydrocarbons are important groups that are involved in heat accumulation during oxidation. Table 4 lists the calculation results.
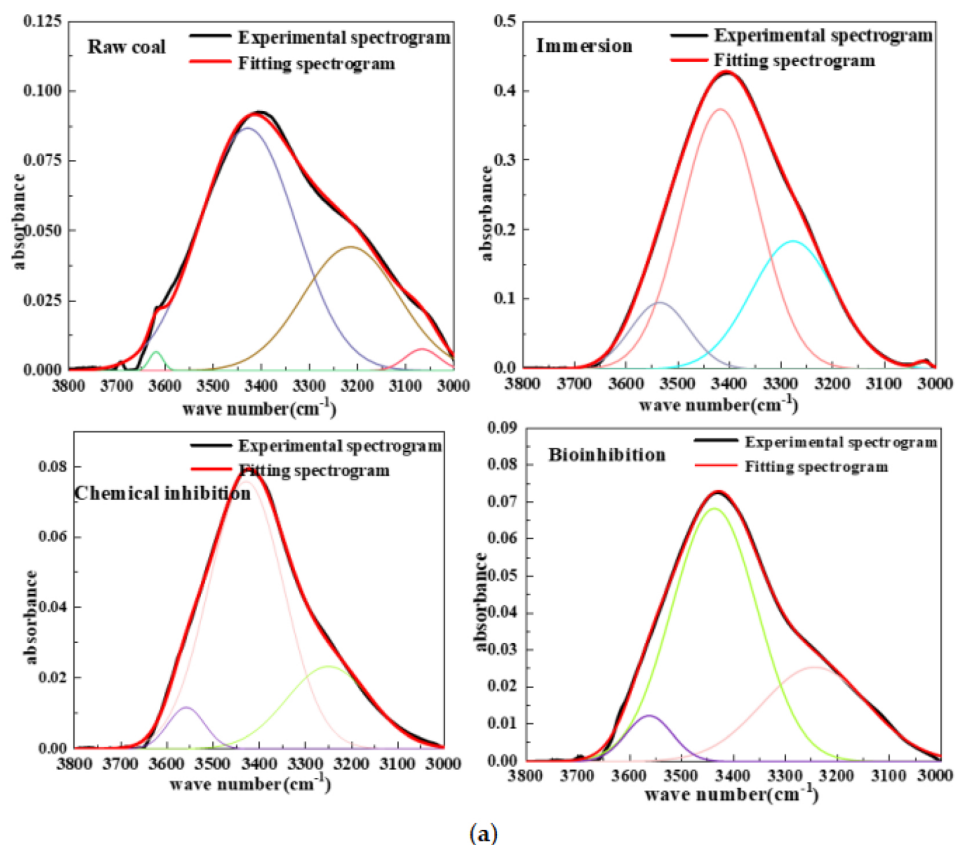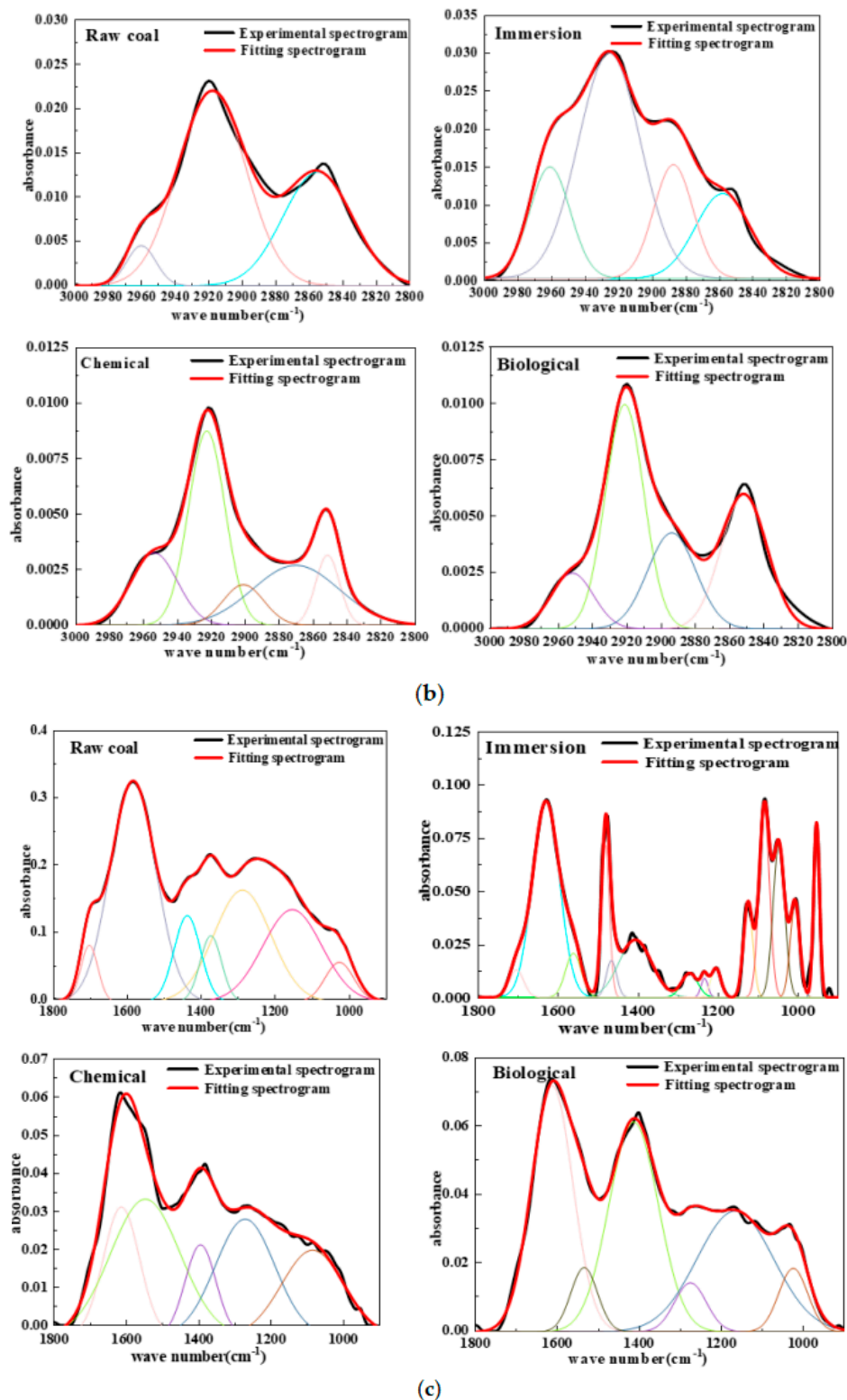

(a)

Figure 7. *Cont.*

Figure 7. Fourier infrared peak fitting diagram of different experimental lignite at different bands. The color lines represent the results of peak division. (**a**) Fourier infrared spectrum peak fitting diagram of 3000~3800 cm^{-1} experimental coal sample. (**b**) Fourier infrared spectrum peak fitting diagram of 2800~3000 cm^{-1} experimental coal sample. (**c**) Fourier infrared spectrum peak fitting diagram of 1000~1800 cm^{-1} experimental coal sample. The four sub-charts in the three groups (**a–c**) show, from left to right and from top to bottom, the lignite raw coal, immersed lignite, chemically inhibited lignite and biologically inhibited lignite in the corresponding bands respectively.

Table 4. Content changes in different active functional groups in coal samples after treatment.

Coal Sample		$D_{-CH3/-CH2}$	D_{-OH}	D_{-COOH}
Lignite	Raw coal	-	-	-
	Bioretarded	−96.6%	−33.5%	−70.7%
	Chemically inhibited	−94.4%	−33.8%	−77.9%
	Immersed	−67.7%	268.2%	−73.3%
Long-flame coal	Raw coal	-	-	-
	Bioretarded	−90.7%	−39.6%	−43.7%
	Chemically inhibited	−92.2%	−21.5%	−42.5%
	Immersed	−73.1%	−4.68	1.20%

Table 4 shows the content changes in the hydroxyl, carboxyl, and aliphatic groups (methyl and methylene) with respect to the three treated experimental coal samples compared with raw coal. It is observed in the table that the content of three active groups in the coal samples with added biological inhibitors is reduced compared to the raw coal, among which the content of methyl and methylene is reduced the most.

Via the above comparative analysis, it is observed that regardless of whether chemical or biological inhibitors are added, the content of the three main active groups in the coal sample decreases, among which methyl and methylene contents in aliphatic hydrocarbons are the most obvious; moreover, these two active groups are also the key groups for heat accumulation in the coal oxidation reaction. The decrease in the content of active functional groups indicates that the number of active groups involved in the reaction also decreases correspondingly, thus reducing the reaction rate. The $D_{-CH3/-CH2}$ of the chemically inhibited and bioinhibited coal samples of lignite is −94.4% and −96.6%, respectively. The $D_{-CH3/-CH2}$ of chemically and biologically retarded long-flame coal samples is −90.7% and −92.2%, respectively. These results indicate that biological inhibitors have better effects on the consumption of these two active groups than chemical inhibitors.

5. Conclusions

In this paper, the modification of lignite before and after the addition of retardants was analyzed from the perspective of microscopic structure, and the change in the flame-retardant performances of lignite treated with two retardants compared with that of raw coal was explored. Via comparisons, it was concluded that the oxidation and self-heating capacity of lignite after microbial retardation was effectively curbed during the initial spontaneous combustion stage, and the retardation performance was better than that of chemical retardants.

(1) Based on SEM images, the changing characteristics of the surface micro-morphology of treated coal samples were analyzed. The surface of lignite is mainly composed of dissolution caves and pores. Compared with raw coal, a large number of deposited calcium carbonate particles are obviously attached to the surface of lignite after resistance treatment, which plays a role in physical oxygen insulation.

(2) The pore size distribution, total pore volume, and specific surface area of lignite after different treatments were studied. The holes of lignite mainly exist in the form of parallel slate-like slits and open-wedge holes on all sides. Based on the pore distribution map, it was observed that the primary pores of lignite can be effectively blocked by microbial inhibitors compared with raw coal.

(3) Based on the fitting results of the infrared spectra of coal samples, three main active groups—hydroxyl group, carboxyl group, and methyl/methylene group—were selected for analysis. The results show that the active group contents of lignite molecules, including the hydroxyl group, carboxyl group, and methyl/methylene group after microbial inhibition is lower than that of raw coal. In particular, the content of methyl/methylene involved in the initial oxidation reaction is reduced by 96.5% compared with the baseline content of raw coal, indicating that the biological inhibitor can simultaneously block the oxidation of the three active groups.

(4) The performance difference between biological and chemical inhibition with respect to coal spontaneous combustion was further compared, and it was observed that calcium carbonate produced via biological inhibition showed a denser spherical distribution than that produced via chemical inhibition, indicating that the adhesion of calcium carbonate produced via biological inhibition was better. Based on the pore size distribution map, it is observed that the total pore volume and specific surface area of the coal sample after biological resistance treatment are more reduced compared to chemical resistance treatments, and the number of pores is significantly reduced. The results show that biological inhibition is more effective than chemical inhibition in preventing the spontaneous combustion of lignite at the physical level. According to the results of NMR experiments, the first three components of the coal sample are aromatic carbon, fatty carbon, and carbonyl carbon. The results of FTIR analyses showed that the consumption effect of biological inhibitors on methyl/methylene was better than that of chemical inhibitors, and the spontaneous combustion effect was improved.

Data Availability Statement: Because the data obtained in this study were the result of paid testing, the participants in this study did not agree to share their data publicly, so supporting data was not available.

Conflicts of Interest: The authors declare no conflict of interest.

References

1. Tao, Y.; Huang, Z.; Zhang, Y.; Ding, H.; Hu, X.; Gao, Y.; Sun, C. Study on the Effect of Oxygen on Free Radical Generation in Coal. *Combust. Sci. Technol.* **2022**, *6*, 1–8. [CrossRef]
2. Xu, L.; Li, Q.; Myers, M.; Chen, Q.; Li, X. Application of Nuclear Magnetic Resonance Technology to Carbon Capture, Utilization and Storage: A Review. *J. Rock. Mech. Geotech. Eng.* **2019**, *11*, 892–908. [CrossRef]
3. Niu, H.; Tao, M.; Bu, Y.; Li, S.; Yang, Y.; Sun, Q.; Mao, Z. Spontaneous combustion characteristics and mechanism of water-immersed and air-dried brown coal. *Energy Sources Part A Recovery Util. Environ. Eff.* **2022**, *44*, 7413–7431. [CrossRef]
4. Yu, S.-L.; Liu, X. Study on Multi-Indicator Quantitative Risk Evaluation Methods for Different Periods of Coal Spontaneous Combustion in Coal Mines. *Combust. Sci. Technol.* **2022**, *9*, 1–4. [CrossRef]
5. Bosikov, I.I.; Martyushev, N.V.; Klyuev, R.V.; Savchenko, I.A.; Kukartsev, V.V.; Kukartsev, V.A.; Tynchenko, Y.A. Modeling and Complex Analysis of the Topology Parameters of Ventilation Networks When Ensuring Fire Safety While Developing Coal and Gas Deposits. *Fire* **2023**, *6*, 95. [CrossRef]
6. Xu, Y.; Dehghanpour, H.; Ezulike, O.; Virues, C. An intelligent gel designed to control the spontaneous combustion of coal: Fire prevention and extinguishing properties. *Fuel* **2017**, *210*, 826–835. [CrossRef]
7. Xue, D.; Hu, X.; Cheng, W.; Wei, J.; Zhao, Y.; Shen, L. Fire prevention and control using gel-stabilization foam to inhibit spontaneous combustion of coal: Characteristics and engineering applications. *Fuel* **2020**, *264*, 116903. [CrossRef]
8. Zhong, Y.; Yang, S.; Hu, X.; Cai, J.; Tang, Z.; Xu, Q. Whole process inhibition of a composite superabsorbent polymer-based antioxidant on coal spontaneous combustion. *Arab. J. Sci. Eng.* **2018**, *43*, 5999–6009. [CrossRef]
9. Xue, D.; Hu, X.; Cheng, W.; Yu, X.; Wu, M.; Zhao, Y.; Lu, Y.; Pan, R.; Niu, H.; Hu, S. Development of a novel composite inhibitor modified with proanthocyanidins and mixed with ammonium polyphosphate. *Energy* **2020**, *213*, 118901. [CrossRef]
10. Zhai, X.W.; Pan, W.J.; Xiao, Y.; Wang, S.R.; Ouyang, L.M. Inhibition of coal spontaneous combustion by an environment-friendly, water-based fire extinguishing agent. *J. Therm. Anal. Calorim.* **2021**, *144*, 325–334. [CrossRef]
11. Zhang, Y.; Xu, J.; Wang, D. Experimental study on the inhibition of primary and secondary oxidation of coal by chlorine salt inhibitors. *Min. Saf. Environ. Prot.* **2015**, *42*, 1–4. [CrossRef]
12. Chi, K.; Wang, J.; Ma, L.; Wang, J.; Zhou, C. Synergistic Inhibitory Effect of Free Radical Scavenger/Inorganic Salt Compound Inhibitor on Spontaneous Combustion of Coal. *Combust. Sci. Technol.* **2022**, *194*, 2146–2162. [CrossRef]
13. Meng, X.; Zhang, G.; Chu, R.; Wu, G.; Gao, M.; Dai, J.; Bai, L. Evolution mechanism of active groups and thermal effectsof Chinese lignite in low-temperature oxidation. *Chem. Eng. Commun.* **2019**, *207*, 861–870. [CrossRef]
14. Zheng, L. Test and analysis on salty retardants performance to restrain coal oxidized spontaneous combustion. *Coal Sci. Technol.* **2010**, *38*, 70–72.

15. Lv, H.; Li, B.; Deng, J.; Ye, L.; Gao, W.; Shu, C.M.; Bi, M. A novel methodology for evaluating the inhibitory effect of chloride salts on the ignition risk of coal spontaneous combustion. *Energy* **2021**, *231*, 121093. [CrossRef]

16. Tang, Y. Experimental investigation of applying MgCl2 and phosphates to synergistically inhibit the spontaneous combustion of coal. *J. Energy Inst.* **2018**, *91*, 639–645. [CrossRef]

17. He, S.; Qi, J.; Zhou, C.; Tang, Y.; Liu, H. Quantum chemistry of metal ions (Na^+, Ba^{2+}, Ca^{2+}) inhibiting the activity of oxygen-containing functional groups in coal. *Coal Mine Saf.* **2023**, *54*, 149–155.

18. Soto, F.; Alves, M.; Valdés, J.C.; Armas, O.; Crnkovic, P.; Rodrigues, G.; Lacerda, A.; Melo, L. Experimental study on thermo-responsive inhibitors inhibiting coal spontaneous combustion. *Fuel Process Technol.* **2018**, *175*, 113–122. [CrossRef]

19. Lanfang, Z. Performance analysis of salt retarders for inhibiting spontaneous combustion of coal oxidation. *Coal Sci. Technol.* **2010**, *5*, 70–72.

20. Zhai, X.; Zhou, Y.; Song, B.; Pan, W.; Wang, J. Comparative study on the inhibiting effect of dissolvable tiny-foam extinguishing agent and chlorine salts on coal spontaneous combustion. *Environ. Sci. Pollut. Res.* **2023**, *30*, 80591–80601. [CrossRef]

21. Deng, B.; Qiao, L.; Wang, Y.; Mu, X.; Deng, C.; Jin, Z. Study on the effect of inorganic and organic sodium on coal spontaneous combustion. *Fuel* **2023**, *353*, 129256. [CrossRef]

22. Wang, J.; Li, K.; Zhang, Y.; Wang, J.; Zhou, C. Experimental study on synergistic inhibition of coal spontaneous combustion by magnesium chloride and carbon/oxygen free radical catcher. *Min. Saf. Environ. Prot.* **2021**, *3*, 6–11+16. [CrossRef]

23. Choi, K.H.; Seo, D.J.; Kim, Y.J.; Cho, S.S.; Han, Y.J.; Yang, I.; Kim, C.W.; Oh, K.; An, J.C.; Park, J.I. Molecular Characteristics of Catalytic Nitrogen Removal from Coal Tar Pitch over γ-Alumina-Supported NiMo and CoMo Catalysts. *Int. J. Mol. Sci.* **2023**, *24*, 11793. [CrossRef] [PubMed]

24. Hongying, X.; Mengmeng, M.; Peng, C. Experimental study on inhibition of spontaneous combustion of coal by composite inhibitor by infrared spectrum. *Saf. Environ. Prot. Min. Ind.* **2019**, *46*, 40–44. (In Chinese) [CrossRef]

25. Zhang, Y.; Shu, P.; Zhai, F.; Chen, S.; Wang, K.; Deng, J.; Kang, F.; Li, L. Preparation and properties of hydrotalcite microcapsules for coal spontaneous combustion prevention. *Process Saf. Environ. Prot.* **2021**, *152*, 536–548. [CrossRef]

26. Pandey, J.; Mohalik, N.K.; Mishra, R.K.; Khalkho, A.; Kumar, D.; Singh, V.K. Investigation of the Role of Fire Retardants in Preventing Spontaneous Heating of Coal and Controlling Coal Mine Fires. *Fire Technol.* **2015**, *51*, 227–245. [CrossRef]

27. Gao, K.; Bick, P.; Suleiman, M.T.; Li, X.; Helm, J.; Brown, D.G.; Zouari, N. Wind Erosion Mitigation Using Microbial-Induced Carbonate Precipitation. *J. Geotech. Geoenviron. Eng.* **2023**, *149*, 04023053. [CrossRef]

28. Wang, Z.; Zhang, N.; Jin, Y.; Li, Q.; Xu, J. Application of microbially induced calcium carbonate precipitation (MICP) in sand embankments for scouring/erosion control. *Mar. Georesour. Geotechnol.* **2021**, *39*, 1459–1471. [CrossRef]

29. Dai, X.; Li, W.; Chen, S.; Zeng, J.; Tong, C.; Zhou, J.; Xiang, T.; Zhang, J.; Li, C.; Ye, Y.; et al. Experimental Study on Coastal Sediment Reinforcement by Induced Carbonate Precipitation by Different Enzyme Sources. *Water* **2023**, *15*, 1484. [CrossRef]

30. Zhou, Y.; Li, S.; Bai, Y.; Long, H.; Cai, Y.; Zhang, J. Joint Characterization and Fractal Laws of Pore Structure in Low-Rank Coal. *Sustainability* **2023**, *15*, 9599. [CrossRef]

31. Brunauer, S.; Emmet, P.H.; Teller, E. Adsorption of gases in multimolecular layers. *J. Am. Chem. Soc.* **1938**, *60*, 309–319. [CrossRef]

32. Barrett, E.P.; Joyner, G.; Halenda, P.P. The determination of pore volume and area distribution in porous substances. Computations from nitrogen isotherms. *J. Am. Chem. Soc.* **1951**, *73*, 373–380. [CrossRef]

33. Wu, G.; Ye, Z.; Zhang, L.; Tang, J. Bituminous Coal Sorption Characteristics and Its Modeling of the Main Coal Seam Gas Component in the Huaibei Coalfield, China. *Sustainability* **2023**, *15*, 9822. [CrossRef]

34. Drozd-Rzoska, A.; Rzoska, S.J.; Kalabinski, J. Energy Calculation and Simulation of Methane Adsorbed by Coal with Different Metamorphic Grades. *ACS Omega* **2020**, *5*, 14976–14989. [CrossRef]

35. Wang, M.; Li, Z.; Liang, Z.; Jiang, Z.; Wu, W. Method Selection for Analyzing the Mesopore Structure of Shale—Using a Combination of Multifractal Theory and Low-Pressure Gas Adsorption. *Energies* **2023**, *16*, 2464. [CrossRef]

36. Dong, X.-W.; Wang, A.; Yaning, M. The microscopic pore structure of coal spontaneous combustion propensity to its effects. *Coal Sci. Technol.* **2014**, *42*, 41–45+49.

37. Kan, H.; Wang, Y.; Mo, W.L.; Wei, X.Y.; Mi, H.Y.; Ma, K.J.; Zhu, M.X.; Guo, W.C.; Guo, J.; Niu, J.M. Effect of solvent swelling with different enhancement methods on the microstructure and pyrolysis performance of Hefeng subbituminous coal. *Fuel* **2023**, *332 Pt 1*, 2023.P1. [CrossRef]

38. Nakashima, Y.; Sawatsubashi, T.; Fujii, S. Nondestructive quantification of moisture in powdered low-rank coal by a unilateral nuclear magnetic resonance scanner. *Int. J. Coal Prep. Util.* **2022**, *42*, 1421–1434. [CrossRef]

39. Cui, B.; Wu, B.; Wang, M.; Jin, X.; Shen, Y.; Chang, L. Structural characteristics of coking coal quality on the quality of the coke research. *J. Coal Chem. Ind.* **2023**, *03*, 106–111.

40. Chen, Y.; Zou, C.; Mastalerz, M.; Hu, S.; Gasaway, C.; Tao, X. Applications of Micro-Fourier Transform Infrared Spectroscopy (FTIR) in the Geological Sciences—A Review. *Int. J. Mol. Sci.* **2015**, *16*, 6227. [CrossRef]